

Tightly Coupled Integration of GPS-PPP and MEMS-Based Inertial System Using EKF and UKF

Mahmoud Abd Rabbou and Ahmed El-Rabbany, Canada

Key words: GPS, Precise Point Positioning, GPS/INS integration, tightly coupled integration

Summary

In this paper, an improved Precise Point Positioning GPS/MEMS-based integrated system is introduced for precise positioning applications. Un-differenced ionosphere-free linear combinations of carrier phase and code measurements are processed. Tropospheric delay, satellite clock, ocean loading, Earth tide, carrier-phase windup, relativity, and satellite and receiver antenna phase-center variations are accounted for using rigorous modeling. Tightly coupled mechanism is adopted, which is carried out in the raw measurements domain. Both Extended Kalman filter (EKF) and Unscented Kalman filter (UKF) are developed to merge the GPS and inertial measurements. The performance of integrated system is analyzed using a real test scenario in downtown Kingston.

It is shown that both Extended Kalman and Unscented Kalman filters have comparable performance. The positioning results of the integrated system show that decimeter-level accuracy is achievable. During the GPS outages, the integrated system showed meter-level accuracy when a 60-second outage was introduced. However, the positioning accuracy was improved to sub-decimeter and centimeter level when 30- and 10-second GPS outages were introduced, respectively.

Tightly Coupled Integration of GPS-PPP and MEMS-Based Inertial System Using EKF and UKF

Mahmoud Abd Rabbou and Ahmed El-Rabbany, Canada

1. Introduction

Currently, the highest accuracy GPS positioning solution is obtained through carrier-phase observables in differential mode, involving two or more receivers. However, the requirement of a base station is usually problematic for some applications as it limits the operational range of the system and increases the system cost and complexity. Recent research shows that comparable positioning accuracy can be achieved through precise point positioning (PPP) technique. PPP use un-differenced or between-satellite single differenced carrier phase and pseudorange observations (Elsobeiey and El-Rabbany 2013).

Unfortunately, accurate GPS positioning solution may not always be available due to GPS outages. To overcome these limitations, GPS can be integrated with a relatively environment-independent system, the inertial navigation system (INS). Currently, most integrated GPS/INS systems are based on differential GPS (DGPS) due to the high accuracy of differential mode (Petovello, 2003 and Nassar, 2003). More recently, GPS-PPP was integrated with a tactical grade IMU to achieve comparable accuracy with that of differential mode (Zhang and Gao, 2007). However, the use of high-end INS is generally limited due to their high cost and size. Recently, micro-electro-mechanical sensors (MEMS) inertial sensors have been developed, which are characterized by their small size and low cost compared with high-end inertial sensors. Generally, however, MEMS inertial sensors have poorer performance and stability compared with high-end INS due to the high noise level and severe biases and drifts affecting them.

This research is aimed to develop a new integrated system based on integrating GPS-based PPP with MEMS accelerometers and fiber optic gyros for precise positioning applications. The proposed integrated system requires rigorous modeling of all errors and biases affecting inertial sensors and GPS observations. We use un-differenced observations for GPS PPP. Inertial sensors biases are accounted for through calibration, while Gaussian-Markov stochastic process model is used to account for the sensor's random errors.

2. Un-differenced ionosphere-free model PPP model

The most common PPP model is the un-differenced ionosphere-free combination of code and carrier phase observations (Hofmann-Wellenhof et. al. 2008). This model eliminates the first order ionosphere delay by combining the observations of L_1 and L_2 . The mathematical model for ionosphere-free PPP can be written as:

$$P_3 = \frac{f_1^2 P_1 - f_2^2 P_2}{f_1^2 - f_2^2} = \rho + c[dt_r - dt^s] + T + c[2.546d_{r1} - 1.546d_{r2}] + c[2.546d^{s1} - 1.546d^{s2}] + e_{p3} \quad (1)$$

$$\phi_3 = \frac{f_1^2 \phi_1 - f_2^2 \phi_2}{f_1^2 - f_2^2} = \rho + c[dt_r - dt^s] + T + c[2.546\delta_{r1} - 1.546\delta_{r2}] + c[2.546\delta^{s1} - 1.546\delta^{s2}] + \bar{\lambda}N + e_{\phi3} \quad (2)$$

where P_1 and P_2 are code measurements on L_1 and L_2 , respectively; Φ_1 and Φ_2 are the carrier phase measurements on L_1 and L_2 , respectively; dt_r and dt^s are the clock errors for receiver and satellite, respectively; d_r and d^s are frequency-dependent code hardware delay for receiver and satellite, respectively; δ_r and δ^s are frequency-dependent carrier phase hardware delay for receiver and satellite, respectively; e_{p3} , $e_{\phi3}$ are relevant system noise and un-modeled residual errors for the un-differenced ionosphere-free combination of the code and carrier-phase measurements, respectively; and $\bar{\lambda}$ are the wavelengths for un-differenced ionosphere-free carrier frequencies; \bar{N} is un-differenced ionosphere-free ambiguity bias; c is the speed of light in vacuum; and ρ is the true geometric range from the antenna phase centre of the receiver at reception time to the antenna phase centre of the satellite at transmission time.

3. GPS/MEMS-based IMU integrated system mechanism

In this paper, the tightly coupled (TC) architecture is implemented adopting a central filter to process GPS raw pseudorange, carrier phase and Doppler measurements and the INS-derived observations to produce estimates of the state vector including position, velocity and attitude. The basic state vector consists of the nine navigation parameter errors, namely three position errors, three velocity errors and three attitude errors. Additional states are added to the INS error model in order to account for the effects of the inertial sensor and GPS errors. The complete state vector consists of 24 states describing the basic state vector (the nine navigation parameter errors) and the inertial sensors errors (bias drift and scale factor).

Knowing the precise GPS satellites ephemeris, the outputs of position and velocity from the INS mechanization are used to predict the pseudorange, phase and Doppler measurements. The corrected GPS pseudorange, carrier phase and Doppler measurements are differenced with the INS-predicted measurements. Then, the estimated filter processes those residuals to estimate the integrated system state vector. Finally, the obtained state estimates are feed backed to the INS mechanization using the closed loop

approach. Both Extended Kalman filter (EKF) and Unscented Kalman filter (UKF) are developed to merge the GPS and inertial measurements.

3.1. Extended Kalman Filter (EKF)

EKF transforms the nonlinear system for both the motion and observation models to linear through linearization process by applying Taylor series expansion and neglecting the second and higher order terms assuming Gaussian distribution density which is applied in Kalman filter (KF) estimation. Generally, EKF gives optimal estimation solution for linear models. In other words, for the integrated GPS/INS system, EKF gives optimal solution for the approximate system (linearized system) rather than the original system (nonlinear system). Using first order Taylor linearization may cause divergence of motion models especially during GPS outages due to the impact of neglecting higher order terms especially when low cost MEMS-based IMU is used.

The prediction step is given by (Jekeli, 2001):

$$\delta \hat{x}_{k,k-1} = \Phi_{k,k-1} \delta \hat{x}_{k-1} \quad (3)$$

$$P_{k,k-1} = \Phi_{k,k-1} P_{k-1} \Phi_{k,k-1}^T \quad (4)$$

The update step is given by (Jekeli, 2001):

$$K_k = P_{k,k-1} H_k^T (H_k P_{k,k-1} H_k^T + R_k)^{-1} \quad (5)$$

$$P_k = (I - K_k H_k) P_{k,k-1} \quad (6)$$

$$\delta \hat{x}_k = \delta \hat{x}_{k,k-1} + K_k (\delta Z_k - H_k \delta \hat{x}_{k,k-1}) \quad (7)$$

where $\delta \hat{x}_{k,k-1}$ is the updated error state vector, $\Phi_{k,k-1}$ is the state-transition matrix, $P_{k,k-1}$ is the variance-covariance matrix for the prediction state, R_k is variance covariance matrix for the measurement state, K_k is the Kalman gain, k is the epoch number, H_k is the design matrix related the measurement vector by the error state vector and δZ_k is the measurement vector.

3.2. Unscented Kalman Filter (UKF)

In UKF, a set of scaled sigma points with appropriate weights is deterministically chosen so as to capture the mean and covariance of this random vector up to a third order accuracy. Consider a random vector x with mean \bar{x} and covariance matrix P_x . The scaled sigma points and the corresponding weights can be defined according to Bergman, (2001) as follows:

1. Initialize with (k=0);

$$\bar{x}_0 = E[x_0] \quad (8)$$

$$P_0 = E[(x_0 - \bar{x}_0)(x_0 - \bar{x}_0)^T] \quad (9)$$

2. Define sigma points;

$$x_{k-1}^i = \bar{x} + \sqrt{(n + \lambda)P_x}, W_i = \frac{1}{2(n + \lambda)} \quad (10)$$

$$x_{k-1}^{i+n} = \bar{x} - \sqrt{(n + \lambda)P_x}, W_{i+n} = \frac{1}{2(n + \lambda)} \quad (11)$$

Where $i=1:n$, are the sigma points and n is the dimension of the state vector. The parameter λ is a scaling parameter.

3. Time update step;

$$x_{k,k-1}^i = f(x_{k-1}^i, u_i) + w_k \quad (12)$$

4. Measurement update;

$$Z_{k,k-1}^i = h(x_{k,k-1}^i), \bar{Z}_{k,k-1} = \sum_{i=0}^{2n} W_i Z_{k,k-1}^i, \bar{x}_{k,k-1} = \sum_{i=0}^{2n} W_i x_{k,k-1}^i \quad (13)$$

$$P_{z_k} = \sum_{i=0}^{2n} W_i (\bar{Z}_{k,k-1} - Z_{k,k-1}^i)(\bar{Z}_{k,k-1} - Z_{k,k-1}^i)^T \quad (14)$$

$$P_{x_{k,k-1}} = \sum_{i=0}^{2n} W_i (\bar{x}_{k,k-1} - x_{k,k-1}^i)(\bar{x}_{k,k-1} - x_{k,k-1}^i)^T \quad (15)$$

$$K_k = P_{x_{k,k-1}} P_{y_k}^{-1} \quad (16)$$

$$\bar{x}_k = \bar{x}_{k,k-1} + K_k \bar{Z}_{k,k-1} \quad (17)$$

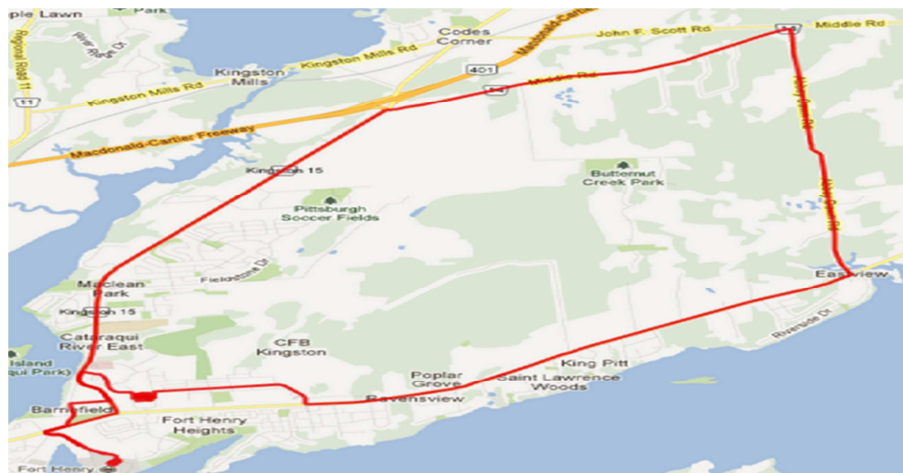
$$P_{x_k} = P_{x_{k,k-1}} - K_k P_{z_k} K_k^T \quad (18)$$

where \bar{x}_0 and P_0 are the initial state vector and variance-covariance matrix respectively. x^i and Z^i are the state and observation vectors for the corresponding sigma points, f and

h are the non-linear motion and observation models respectively. $x_{k,k-1}$, $Z_{k,k-1}$ and $P_{x_{k,k-1}}$ are the time prediction state vector, observation vector and variance-covariance matrix respectively. x_k , and P_{x_k} are the time update state vector variance-covariance matrix respectively.

Vehicular test is conducted to evaluate the performance of the developed integrated GPS-PPP/MEMS-based IMU system. The vehicular test was carried out in downtown Kingston, Ontario (Figure 1). The test location represents difficult scenarios for satellite navigation, with frequent partial GPS outages of several seconds. Novatel SPAN-CPT system is used for obtaining the inertial data records and Trimble R10 receiver is employed for obtaining GPS observations. The SPAN-CPT system consists of a Novatel OEM4 receiver and MEMS IMU consisting of three MEMS-based accelerometers and three fiber optic gyros. Only the performance of the positioning accuracy is considered in this paper. The positioning results of the integrated system show that decimeter-level accuracy is achievable for both EKF and UKF. To simulate the challenging conditions of the trajectory trip including high and slow speeds, twelve simulated GPS outages of 60s, 30s and 10s are introduced. Both EKF and UKF have similar accuracy-level during the outages.

Figures 2, 3 and 4 show the positioning errors referenced to carrier-phase-based DGPS solution for latitude, longitude and altitude. The results show decimeter-level positioning accuracy for both EKF and UKF. Figure 5 shows the root-mean-square error (RMSE) and the maximum errors of the positioning results. Figure 6 shows the accuracy of the integrated system during various complete GPS outages. As can be seen, the integrated system shows meter-level accuracy when a 60-second outage is introduced. However, the positioning accuracy is improved to sub-decimeter during 30- and 10-second GPS outages, respectively.



Tightly Coupled Integration of GPS-PPP and MEMS-Based Inertial System Using EKF and UKF (7269)

Mahmoud Abd Rabbou and Ahmed El-Rabbany (Canada)

Figure 1. Trajectory test area

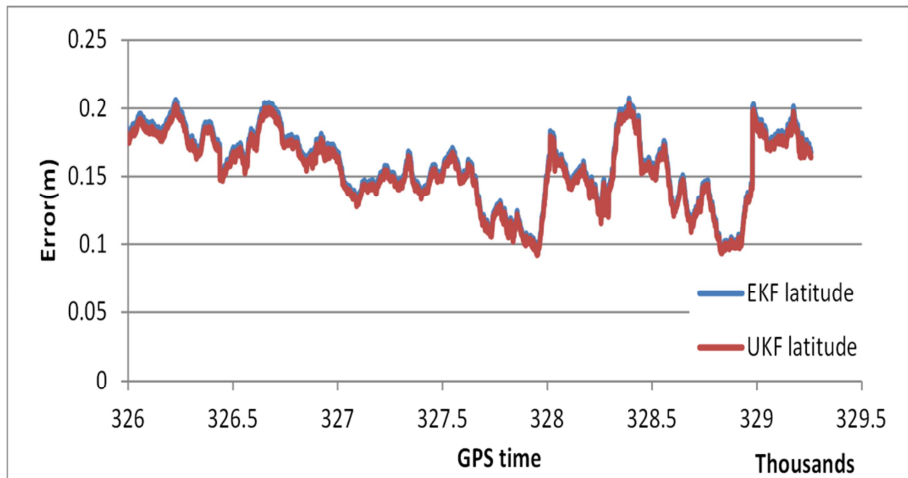


Figure 2. Latitude accuracy using EKF and UKF

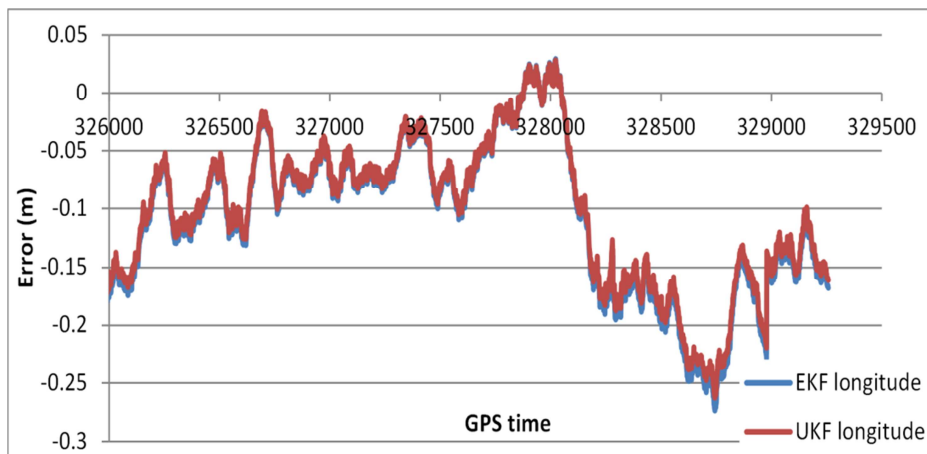


Figure 3. Longitude accuracy using EKF and UKF

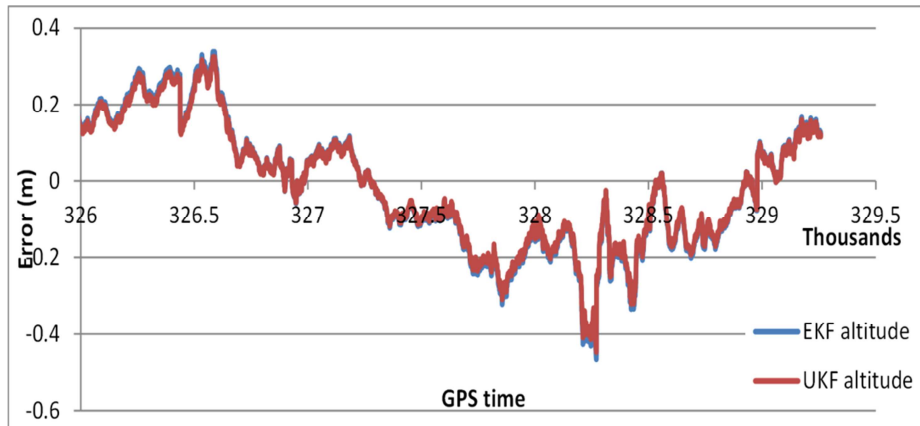


Figure 4. Altitude accuracy using EKF and UKF

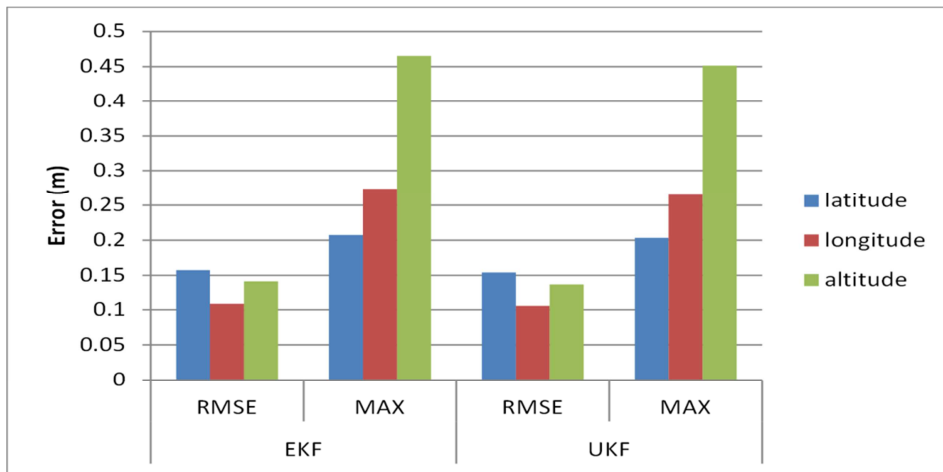


Figure 5. Maximum and RMSE errors for EKF and UKF

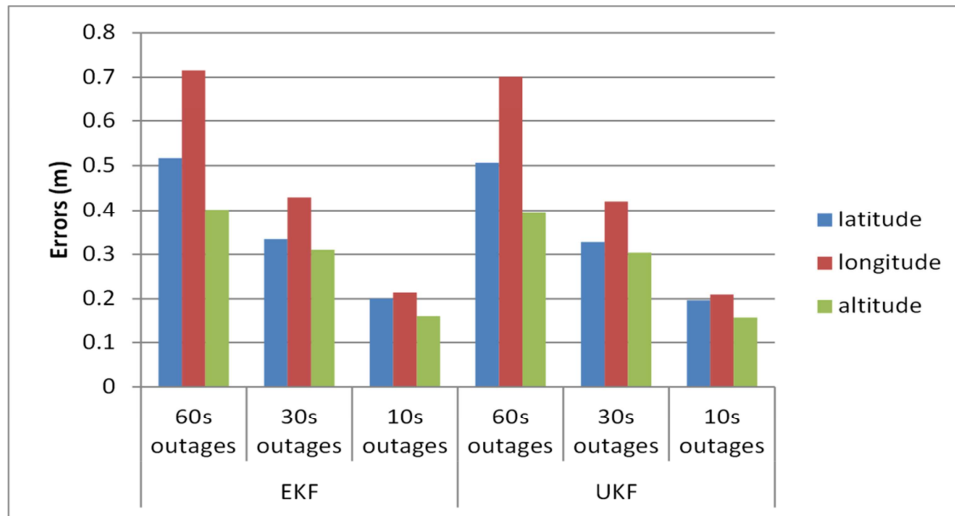


Figure 6. The average of max positioning errors during GPS 60 sec, 30 sec and 10 sec outages using EKF and UKF

4. Conclusion

This research developed new algorithms for the integration of GPS PPP and MEMS-based IMU. Tightly coupled mechanization was implemented using both EKF and UKF. The performance of integrated system was analyzed using a real test scenario in downtown Kingston, Ontario. Undifferenced ionosphere-free linear combinations of code and carrier-phase measurements were considered. The positioning results of the integrated system showed that decimeter-level accuracy is achievable for both EKF and UKF. During the GPS outages, the integrated system showed meter-level accuracy when a 60-second outage was introduced. However, the positioning accuracy was improved to sub-decimeter and centimeter level when 30- and 10-second GPS outages were introduced, respectively. These results are very encouraging as they are comparable to high-end differential-based GPS/INS systems.

5. References

- Bergman, N. (2001). Posterior Cramer-Rao Bounds for Sequential Estimation, in Sequential Monte Carlo methods in practice (A. Doucet, N. de Freitas, and N. Gordon, eds.). pp. 321–338, New York: Springer Verlag.
- Elsobeiey, M. and El-Rabbany, A. (2013). Efficient Between-Satellite Single-Difference Precise Point Positioning Model. *Journal of Surveying Engineering.*, 10.1061/(ASCE)SU.1943-5428.0000125 , 04014007.
- Hofmann-Wellenhof, B., H. Lichtenegger, and E. Wasle. (2008). GNSS Global Navigation Satellite Systems; GPS, GLONASS, GALILEO & more. Springer Wien New York.

- Jekeli, C. (2001). Inertial navigation systems with geodetic applications, Berlin, New York, de Gruyter. ISBN 3-11-015903-1.
- Nassar, S. (2003). Improving the Inertial Navigation System (INS) Error Model for INS and INS/DGPS Applications. PhD Thesis, Department of Geomatics Engineering, University of Calgary, Canada,
- Petovello, M. (2003). Real-time Integration of a Tactical-Grade IMU and GPS for High-Accuracy Positioning and Navigation. PhD Thesis, Department of Geomatics Engineering, University of Calgary, Canada, UCGE Report No. 20173.
- Zhang, Y., and Gao, Y. (2007). Integration of INS and Undifferenced GPS Measurements for Precise Position and Attitude Determination. *The Journal of Navigation*, 61, The Royal Institute of Navigation, pp.1-11.

Biography – Mahmoud Abd El-Rahman

Mahmoud obtained his B.Sc. and M.Sc. degrees from the Department of Civil Engineering at Cairo University in 2007 and 2010, respectively. He worked as an assistant lecturer of civil engineering at Cairo University since graduation. In 2011, he joined the Geomatics research group in the Department of Civil Engineering, Ryerson University, as a Ph.D. student. His research focuses on navigation system technology, global navigation satellite systems (GNSS), and GNSS/INS integration.

Biography - Ahmed El-Rabbany

Dr. Ahmed El-Rabbany obtained his PhD degree in GPS Satellite Navigation from the Department of Geodesy and Geomatics Engineering, University of New Brunswick, Canada. He is currently a full professor and Graduate Program Director at Ryerson University, Toronto, Canada. He also holds an Honorary Research Associate position at the University of New Brunswick. Dr. El-Rabbany's areas of expertise include Satellite Navigation, Geodesy and Hydrographic Surveying. He is an Associate Editor of *Geomatica* and Editorial Board member for the *Journal of Navigation* and the *AIN Journal*. He also holds the position of President-Elect with the Canadian Institute of Geomatics. Dr. El-Rabbany received numerous awards in recognition of his academic achievements, including three merit awards and distinguished service award from Ryerson University and best papers and posters at various conferences and professional events. He was also honoured by a number of academic and professional institutions worldwide.

CONTACTS

Mahmoud Abd Rabbou
Ryerson University
350 Victoria Street
Toronto, Ontario
CANADA
Tel. +1 (647)774-6799
Email: Mahmoud.abdelrahman@ryerson.ca

Dr. Ahmed El-Rabbany, P.Eng.
Ryerson University
350 Victoria Street
Toronto, Ontario
CANADA
Tel. +1 (416) 979-5000 ext. 6472
Fax +1 (416) 979-5122
Email: rabbany@ryerson.ca
Web site: <http://www.civil.ryerson.ca>